

Decagonal Quasicrystal Tilings

BY R. INGALLS

Department of Physics, FM-15, University of Washington, Seattle, WA 98195, USA

(Received 9 October 1991; accepted 24 January 1992)

Abstract

A description is given of three new distinct quasiperiodic tilings that exhibit tenfold symmetry. Related to each other by decomposition, these tilings are most easily generated from their respective Fibonacci pentagrid dual tilings. The latter, one of which is singular, are based on the property that there are three principle Fibonacci quasiperiodic sequences that possess mirror symmetry. The resulting tilings, while somewhat analogous to the Penrose tilings, are more complex in that they contain inequivalent tiles of the same shape. Associated with each of these decagonal tilings, which belong to different local isomorphism classes, are one twofold and two different fivefold tilings. Twelve inflations or deflations are necessary before each of the latter reoccurs with the same orientation.

Introduction

In the last few years, considerable attention has been given to quasicrystal tilings, including the pentagonal plane tilings due to Penrose (Penrose, 1974; Gardner, 1977; Grünbaum & Shepard, 1986). Such study (Levine & Steinhardt, 1986), with its extension to other dimensions and point symmetries (Socolar, 1989), was greatly spurred on by the discovery of icosahedral (Schechtman, Blech, Gratias & Cahn, 1984) and decagonal (Bendersky, 1985) phases of metallic alloys. It has led to several methods whereby one can now generate an infinite variety of such theoretical structures in a straightforward way (Socolar & Steinhardt, 1986). Here one such approach is taken, namely, the dual method (de Bruijn, 1981; Kramer & Neri, 1984), and is used to generate three significant tilings of perfect tenfold symmetry and infinite extent. One infinite twofold and two infinite fivefold tilings, associated with each of the tenfold patterns, are also described. Also discussed is the important relationship of these new tilings to those of Penrose and, more directly, to the three-dimensional zonohedral tilings proposed as a natural framework for the icosahedral alloys (Socolar & Steinhardt, 1986).

Pentagrids and duals

Penrose patterns are ideal infinite aperiodic tilings that have the property of deflation (or inflation) whereby they can be decomposed into similar smaller (or larger) tiles, which fit together in the same way as in the original version (Gardner, 1977). Since the deflated or inflated tilings possess the same local environments, apart from a scale factor, as the original, they are said to be of the same 'local isomorphism' class (Levine & Steinhardt, 1986). Each successive deflation or inflation leads to tiles that are smaller or larger by a factor $\tau = (1 + \sqrt{5})/2$, the golden mean. Moreover, one way of marking the tiles to ensure aperiodicity when they are joined together is simply to imprint them with one of the deflated patterns into which they can be subdivided. However, another important way of decorating the tiles is with line segments such that, when the tiles are properly joined, continuous straight lines, the 'Ammann lines', result (Grünbaum & Shepard, 1986), forming five overlapping parallel-line grids. Each of these grids is perpendicular to one of five principal directions in the plane and together they form a 'pentagrid' (de Bruijn, 1981).

Pentagonal tilings generalized from the Penrose rhombic pattern generally consist of two shapes, namely a thick rhomb and a thin one, with the edges of the tiles parallel to one of the above principal directions. Many can be shown to be dual to a pentagrid and can be derived from it in a straightforward way (de Bruijn, 1981). That is, each open space in a pentagrid can correspond to the corner of a rhomb in the dual tiling. Going from one space to another, that is, crossing a grid line, then corresponds to a unit step perpendicular to that line, *i.e.* the edge of a tile. Conversely, each intersection in the pentagrid corresponds to a tile itself. If the acute angle at an intersection is 36° , the rhomb is thin, whereas an angle of 72° leads to a thick rhomb. Interestingly, with a Penrose tiling the characteristic Ammann-line decoration associated with its parent (the tiling inflated by one order) serves as its pentagrid dual (Socolar & Steinhardt, 1986). Moreover, the spacing within each of the five grids forming this pentagrid is related to the quasiperiodic Fibonacci sequence (de Bruijn, 1981; Grünbaum & Shepard, 1986), a special sequence of long and short spaces. However, the

Penrose pattern can also be generated from a periodic pentagrid dual (Socolar & Steinhardt, 1986). Moreover, as will be discussed later, generally more than one Ammann-line decoration exists for the same tiling. Analogous statements apply to tilings of other symmetries (Socolar, 1989).

The dual method can be generalized. For instance, the line spacing within a grid can be arbitrary, as can the direction of its normal. In three dimensions, a grid would consist of parallel planes and the tiles corresponding to the intersection of three planes would be rhombohedra (Socolar & Steinhardt, 1986). The possibilities are endless. Here we primarily examine some other especially significant tilings, besides Penrose's, that can result from Fibonacci pentagrid duals. As a guide to this approach, we first study several generations of the Fibonacci sequence itself, since each Fibonacci grid within a pentagrid inflates or deflates in a prescribed way (Grünbaum & Shepard, 1986). Through the dual method, the inflation or deflation schemes for the associated tilings can then be found. The Fibonacci sequence is of course itself the prototype of a one-dimensional quasicrystal. In Fig. 1 we show successive deflations of a long spacing, L . As shown, $L \rightarrow L/2$, s , $L/2$ and $S \rightarrow L/2$, $L/2$. Thus a short space in the parent pattern is equal in length to a long space in the deflated pattern. Similarly, a long space becomes a long-plus-short space when deflated. Also, since $L/S = \tau$, this rule leads to successive generations that differ in scale by that same factor.

The rhombic tiling derived from Penrose's 'infinite cartwheel' pattern (Gardner, 1977), originally composed of kites and darts, is shown in Fig. 2. This pattern is especially appropriate for illustrating the above properties because its deflated version is simply a smaller replica of the same tiling, but rotated about the center, C , by 180° . The deflated pattern is either obtained by decomposition or by simply taking the dual of the Ammann-line pentagrid decoration shown superposed on the tiling. However, this pentagrid is composed of five identical Fibonacci grids whose centers correspond to the line in Fig. 1 labeled c . These sequences, like the tiling itself, reverse with each deflation, so, for instance, the second generation is identical to the parent (zeroth generation), apart from the reduction by the factor τ^2 . The tiling in Fig. 2 is itself the dual to the pentagrid based on the

sequence c in Fig. 1, whereas the Ammann-line pentagrid in Fig. 2 is based upon the sequence \bar{c} . The various pentagrids discussed in this paper are given in the Appendix (Fig. 7) with the same labels as the corresponding Fibonacci sequences in Fig. 1.

It is remarkable that, except for the central SL , the Fibonacci sequence c , corresponding to the cartwheel pattern, *i.e.* $-LLSLSLLSLL-$ is completely symmetric about its center (Grünbaum & Shepard, 1986). Otherwise, the resulting tiling would have perfect tenfold symmetry rather than the tenfold pseudosymmetry that is its hallmark. The reason the cartwheel actually only possesses left-right (mirror) symmetry, rather than fivefold, is that two of the grids are reversed. (Considering our principal directions to be every 72° starting from the top of the page, these reversed grids are those normal to the $\pm 72^\circ$ directions.)

Slightly more complex behavior is found in the regions in Fig. 2, labeled S and S' (or their rotated versions, \bar{S} and \bar{S}'), having local fivefold symmetry, one type leading to the other upon deflation. These regions, of course, serve as nuclei for patterns that are the rhombic versions of Penrose's 'infinite sun' or 'infinite star' kite and dart patterns (Gardner, 1977). It is evident that the regions S (or \bar{S}) in Fig. 2 are generated from corresponding Ammann-line duals in the neighborhood of S' (or \bar{S}') and *vice versa*. Locally, each of these pentagrids is composed of five identical Fibonacci grids, the center of each corresponding to the line marked s (for sun, star) in Fig. 1. In particular, deflation along s in Fig. 1 yields the grid sequences labeled s and then s' , followed by \bar{s} and \bar{s}' , before the whole process repeats. The same would apply to the corresponding infinite fivefold tilings themselves. This illustrates why one has the deflation chain: sun, star, rotated sun, rotated star, sun *etc.* in the original Penrose tilings (Grünbaum & Shepard, 1986). Thus, starting with a particular fivefold tiling, two orders of deflation cause 180° rotation (and a change in the scale by a factor of τ^2) but the pattern does not truly repeat in orientation as well until the fourth generation.

New tilings with tenfold symmetry

In addition to the above, there are other important symmetry points associated with the Fibonacci sequence that can lead to tilings comparable to

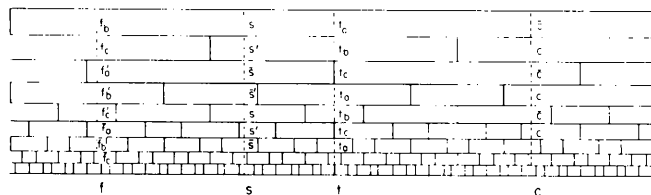


Fig. 1. The quasiperiodic Fibonacci sequence. The special inflation/deflation chains f , s , t and c are discussed in the text.

Penrose's. For instance, it is apparent from Fig. 1 that there are three kinds of sequences that, in fact, do have perfect mirror symmetry. They are associated with the line marked t . Thus a pentagrid composed of one of the above grid types, properly centered, would yield a dual tiling possessing true tenfold symmetry. Pursuing this, we first consider such a pentagrid based on the sequence in Fig. 1 labeled t_a , $-SLLSLLS-$. The resulting infinite tenfold tiling dual to this pentagrid, which we label T_a in Fig. 3(a), is seen to be centered about a 'flower' of ten thin rhombs. Although there are an infinite number of such flowers in the extended pattern, only the central one can be a point of true tenfold symmetry. The salient properties of this pattern such as inflation/deflation, Ammann lines, matching rules, inequivalent cells of the same shape and the possible twofold tilings, or fivefolds derived from the star arrangements, remain to be examined.* Before doing so, however, the two remaining tenfolds based on the central line t in Fig. 1 will first be obtained.

Therefore, proceeding to the dual of the pentagrid derived from the symmetric sequence t_b , *i.e.* $-LSLLSLLS-$, the deflation of t_a , one arrives at the second tenfold tiling T_b in Fig. 3(b). For now, it is simply noted that although this second tiling also has flowers and stars, it is clearly not locally isomorphic to T_a . Continuing down line t in Fig. 1, one may construct the pentagrid based on the sequence t_c , consisting of the symmetric $-LSLSLLS-$. This pentagrid is remarkable in that it contains many inter-

* Of course, as in the Penrose case, infinite tilings of no particular symmetry may be obtained by expanding about an arbitrary point *via* deflation.

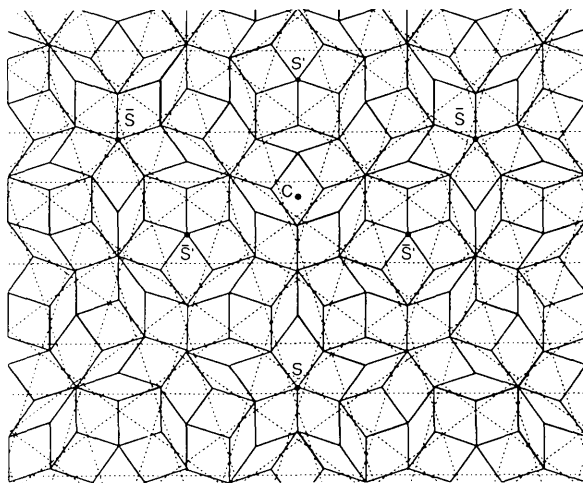


Fig. 2. Rhombic version of Penrose's infinite cartwheel tiling. Also shown is the corresponding Ammann-line pentagrid decoration (dotted lines). The point C marks the center, while S and S' etc. mark points of local fivefold symmetry, related to Penrose's infinite sun and infinite star patterns.

sections of more than two grid lines. For this reason, such a pentagrid has been termed 'singular' (de Bruijn, 1981). It is unique in that tiles generated from it *via* the dual method are not only rhombs but also hexagons, octagons and decagons, corresponding to intersections of three, four or five Ammann lines, respectively. The actual tiling by such shapes, T_c , derived from this singular pentagrid and sequence t_c , is shown in Fig. 3(c). It is seen to consist of four different shapes, a thick rhomb, a thick hexagon, an octagon and a decagon. In fact, of the possible polygons, only the thin rhomb and thin hexagon are absent from this striking pattern. (The thin hexagon would be equivalent to one thick and two thin rhombs, whereas the thick hexagon decomposes into one thin and two thick rhombs.)

It is a general characteristic of all three patterns that, as one moves out from the true center, the local tenfold regions resemble the infinite tenfold pattern to a greater and greater extent. A corresponding statement applies to the local two- and fivefold regions which more and more resemble the infinite two- and fivefold patterns discussed in the next section. The Penrose tilings, of course, possess this same general property (Gardner, 1977).

The chain $-t_a, t_b, t_c, t_a-$ in Fig. 1 leads to the deflation of the tenfold tilings in the order $-T_a, T_b, T_c, T_a-$ with the lengths of the tile edges decreasing each time by the factor τ . [In Fig. 3(a), tiling T_a is a factor of τ smaller than this scheme so that more of it may be shown.] In contrast to the Penrose case, however, each succeeding deflation leads to a tiling that is in a different local isomorphism class. Yet with each third generation in the deflation/inflation hierarchy, the same tiling reappears, identical except for a scale factor of τ^3 . Clearly, therefore, the tilings may be decorated with any deflated tiling or any of the three Ammann-line pentagrids, suitably scaled. Some of the many possibilities are shown in Fig. 4. A portion of tiling T_c decorated with one of the next three successive tilings, namely T_a, T_b and T_c itself, is shown in Figs. 4(a)-(c). It is thus apparent that a third-generation marking of T_c as in Fig. 4(c) provides a miniature plan for easily continuing the tiling to infinity, quite analogous to marking the cartwheel by its second-generation deflation. If the small tiles in Fig. 4(c) are in turn decorated as in Figs. 4(a) and (b), the other two infinite tilings may also be readily obtained. Of course these tilings too may be decorated with a miniature τ^3 replica. (This type of decoration is shown in Fig. 6 of the next section.)

As in the Penrose case, the pentagrid dual from which each tiling is generated serves as the canonical Ammann-line decoration for the next tiling higher in the inflation hierarchy (Socolar & Steinhardt, 1986). This is indicated by the dotted lines in Figs. 4(a), (b) and (d), where T_a, T_b and T_c are decorated with

pentagrids based on the Fibonacci sequences t_b , t_c and t_a respectively. However, the other pentagrids can also serve as Ammann-line decorations for the three tilings. For example, the singular pentagrid based upon sequence t_c is a particularly pleasing decoration [dashed lines in Figs. 4(b) and (c)]. When used for T_c , its dual, each tile contains the appropriate multiple-line intersection that generated it. However, the other tilings are not quite as transparently marked by their respective duals.

The various decorations of these three new patterns not only establish matching-rule schemes but also enable one to distinguish inequivalent tiles. Using the above procedures for T_a leads to two inequivalent thin and, as in Fig. 4(a), five inequivalent thick rhombs. In the case of T_b , there are one thin and three inequivalent thick rhombs. For T_c , all decagons, octagons and hexagons are equivalent. However, there appear to be two inequivalent thick rhombs [Figs. 4(a) and (d) and the small tiles in Fig. 4(c)].

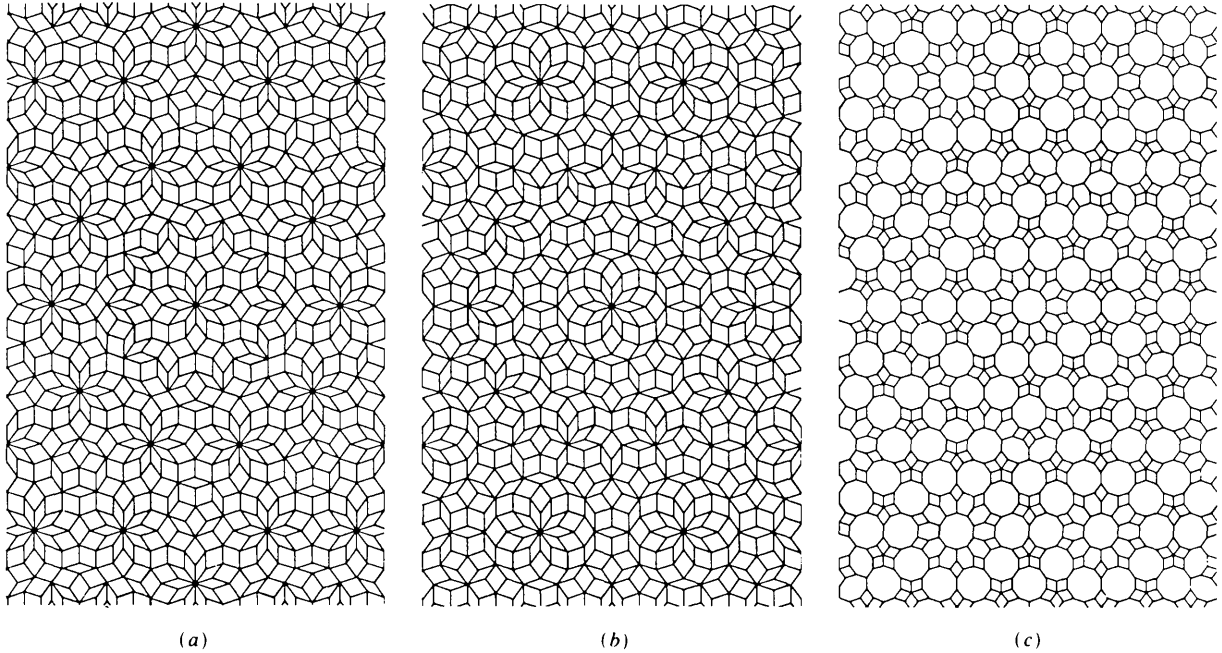


Fig. 3. The three infinite tenfold tilings, dual to pentagrids based on respective Fibonacci sequences in Fig. 1, centered about the line labeled t . (a) T_a , (b) T_b and (c) T_c .

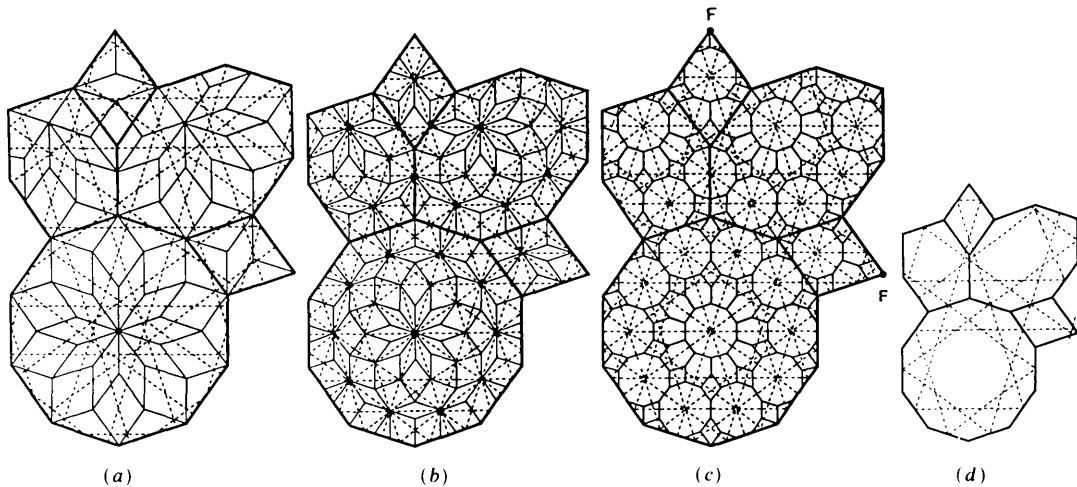


Fig. 4. Several decorations of the tiles of T_c . (a) Tiling T_a and pentagrid t_b , (b) tiling T_b and pentagrid t_c , (c) tiling T_c and pentagrid t_c and (d) pentagrid t_a . In each case, the Ammann-line pentagrid decoration is indicated by dotted lines.

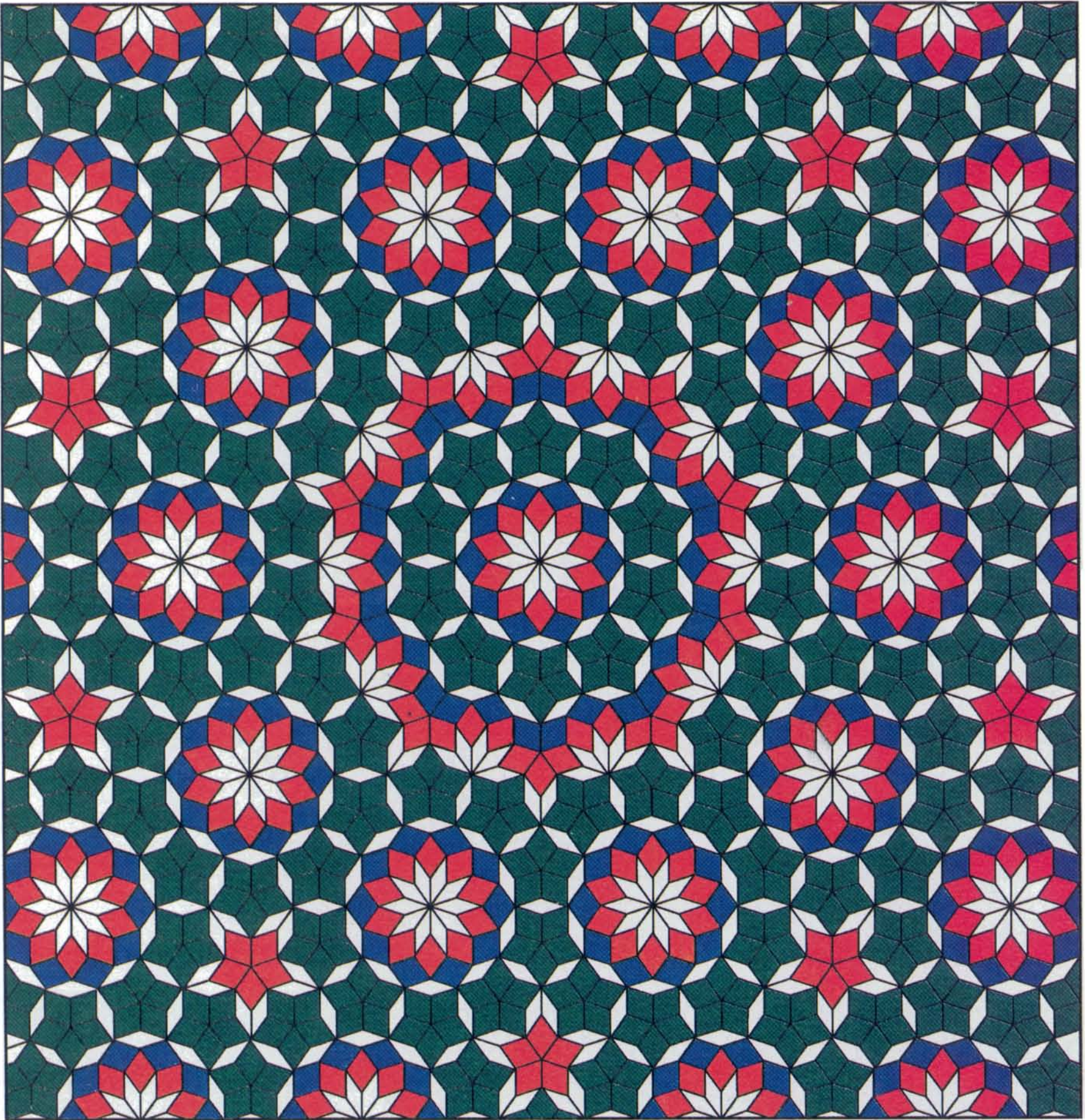


Fig. 5. Decagonal tiling T_b , with its three inequivalent thick rhombs indicated by different colors.

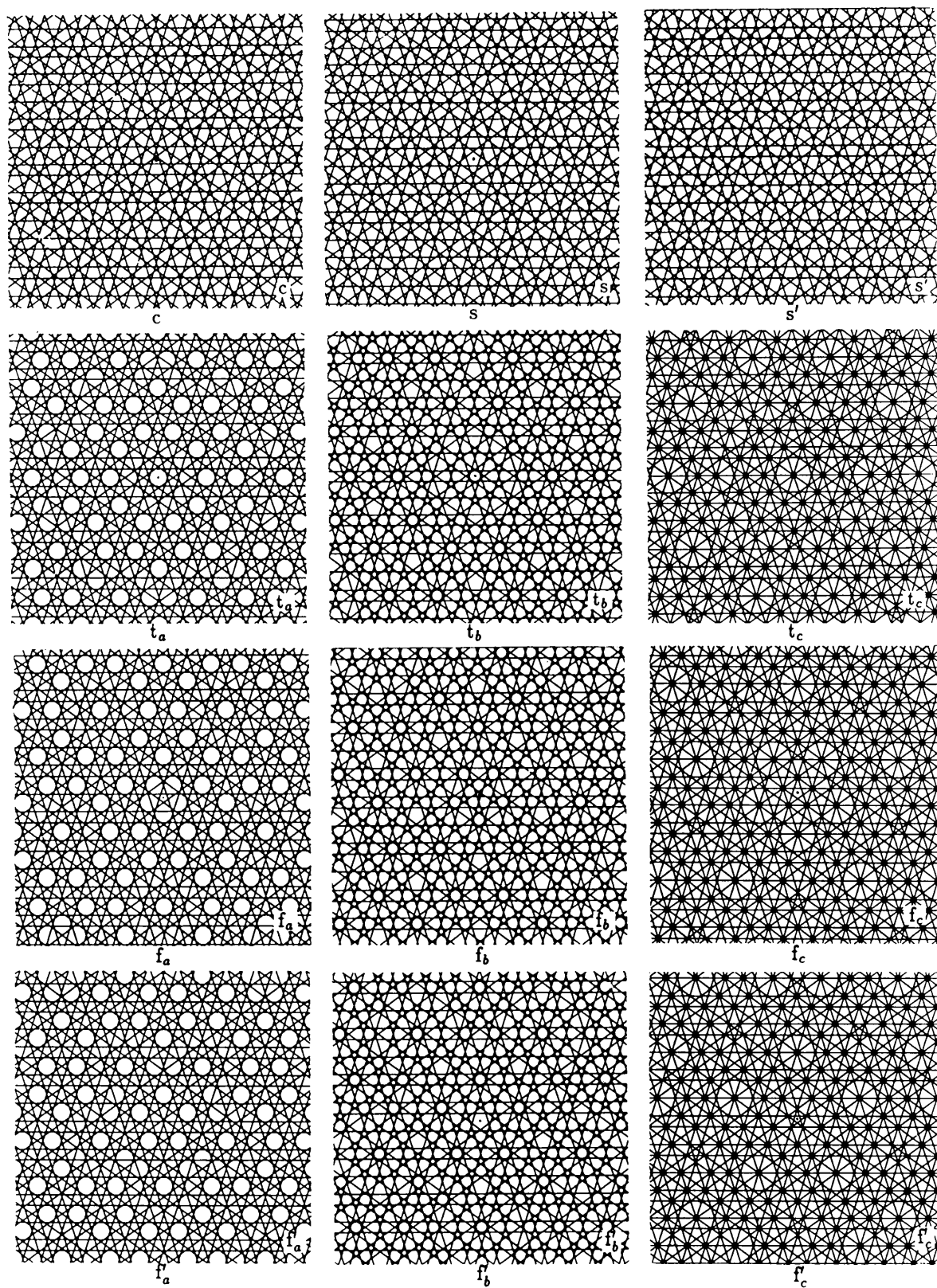


Fig. 7. The various Fibonacci pentagrids that are dual to the tilings discussed in this work.

The actual number of inequivalent tiles depends upon the decoration. As the latter becomes more deflated and less coarse, some of the inequivalency disappears. This is evident in the decorations of the large tiles in Figs. 4(b) or (c), where the two thick rhombs have the same decoration. Similarly, with a finer decoration, the two types of smaller thick rhombs forming the completed stars in Fig. 4(a) would appear equivalent. This behavior appears to be universal for those tilings, including Penrose's, that are amenable to decomposition. A natural coloring scheme then would be simply to assign different colors to inequivalent tiles. Tiling T_b is treated this way in Fig. 5. Based on the results here, it is conjectured that all inequivalent tiles, rather than a subset, are required to form a tiling.

It is readily apparent from Fig. 4 and Fig. 6 of the next section that the deflation and Ammann-line

decorations both offer consistent sets of matching rules that ensure quasiperiodicity. The rule for the Ammann lines is that not only do all lines join to form straight lines, but they join to form a Fibonacci pentagrid. Without the latter restriction, the thin rhombs in Fig. 4(b) could be joined in a periodic manner. However, in accordance with the previous discussion, finer decorations, such as in Fig. 6, or decoration with deflated pentagrids t_a , t_b or t_c itself, would prevent a periodic arrangement.

It is noted here that another infinite tenfold rhombic pattern has appeared in the literature (Conway & Knowles, 1986), generated from higher-dimensional space *via* the projection technique. It somewhat resembles T_a or T_b and can be shown to be dual to a periodic pentagrid, *i.e.* one where the center of the grid pattern lies halfway between two of the lines in each identical periodic grid. That

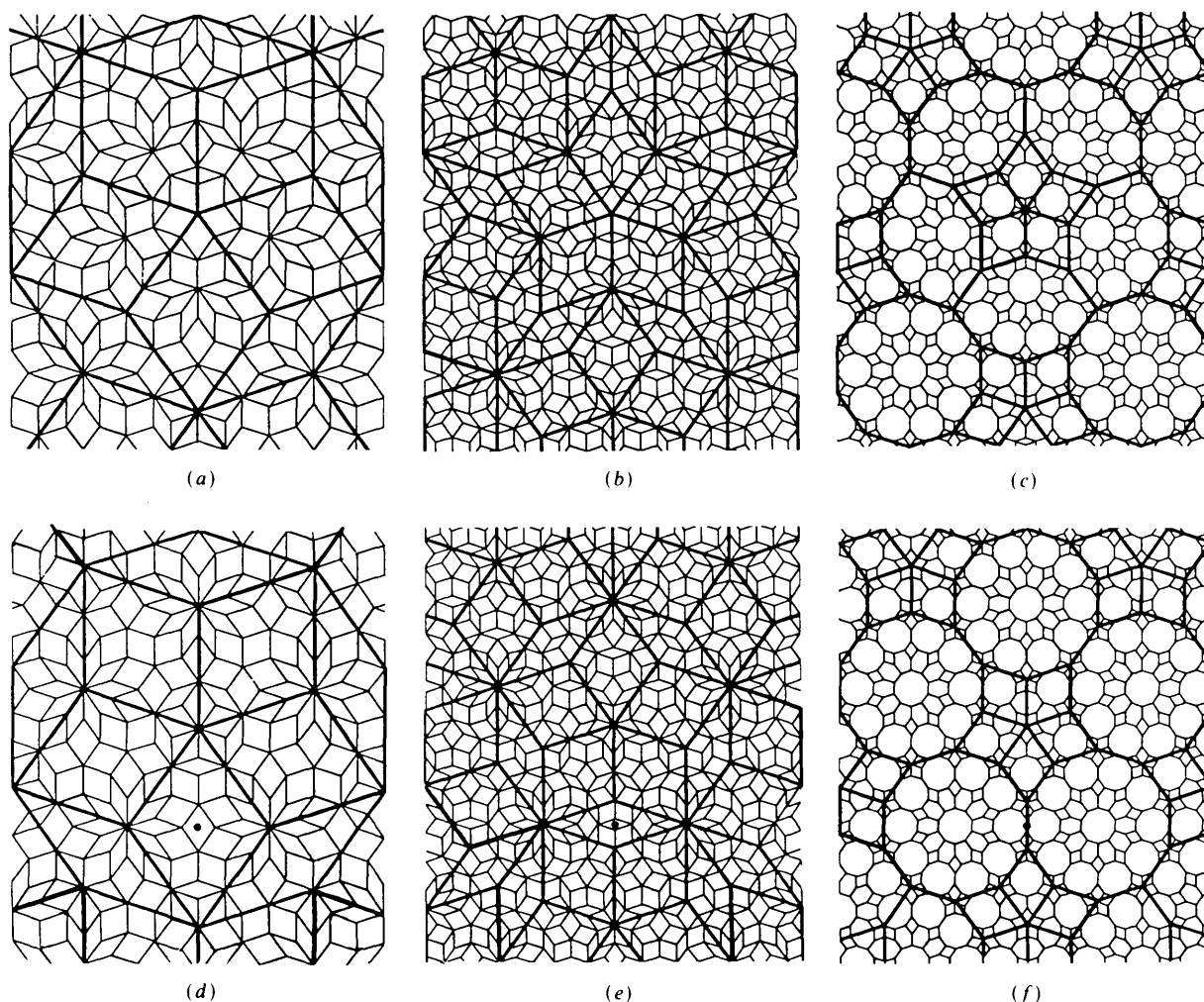


Fig. 6. Three pairs of infinite fivefold patterns locally isomorphic to the respective tilings of Fig. 3. They are also dual to pentagrids based on the respective Fibonacci sequences in Fig. 1 centered about the deflation line, labeled f. Superposed are representative tiles associated with the τ^3 third-order inflation in each case. A dot slightly below each fivefold center in (d)-(f) indicates a nucleation point for the infinite twofold pattern.

particular pattern appears to have the greatest density of local tenfold points (flowers) obtainable by projection (Ishihara & Yamamoto, 1988). However, the density of flowers in the tiling T_a is higher by a factor of τ^2 , albeit at the expense of having a few of the inequivalent thick rhombs joined in a crystallographic manner. The only other possible periodic pentagrid consistent with tenfold symmetry is singular, with five grid lines passing through the origin. Its dual may be described as essentially the rhombic cartwheel pattern, except for a decagon replacing the central cartwheel cluster and the spokes of the cartwheel, the 'worms', replaced by chains of thick and thin hexagons. It is known (*cf.* Socolar & Steinhardt, 1986) that duals of periodic pentagrids are equivalent to projections from five-dimensional hypercubic lattices. Therefore, it is evident that the three new tenfold tilings described in this paper cannot be obtained by means of such a projection.

Related two- and fivefold tilings

As with the Penrose patterns (Gardner, 1977; Grünbaum & Shepard, 1986), each of the above tilings contains two kinds of regions that can lead to different infinite fivefold tilings. These are most easily generated by starting with either of the two possible stars formed with five identical thick rhombs from the T_c tiling (Fig. 4c) and expanding outward using one of the possible deflation decorations to ensure proper matching. [The points that become fivefold centers are labeled F in Fig. 4(c).] By using the T_a and T_b decorations (Figs. 4a and b), four more patterns are formed. These tilings, six in all, are shown in Fig. 6 together with their respective τ^3 third-order-inflation supertilings superposed. The deflation sequence is as follows: $F_a, F_b, F_c, F'_a, F'_b, F'_c$, and then the same order again but with each tiling rotated by 180° *etc.* The respective supertilings are, of course, $\bar{F}'_a, \bar{F}'_b, \bar{F}'_c, F_a, F_b$ and F_c *etc.* In Figs. 6(d)–(f), the tilings have been increased in size by the factor τ^3 , so the supertiles correspond to the small tiles in Figs. 6(a)–(c), respectively.

Similar to the preceding cases, one can identify points in the Fibonacci sequence that correspond to the centers of the pentagrid duals associated with these fivefold patterns. These points are labeled f in Fig. 1 with the associated Fibonacci sequences labeled f_a, f_b *etc.*, respectively. Therefore, although the same local isomorphism class appears every third generation, the same basic tiling, rotated, reappears every sixth generation. Therefore, it takes twelve generations before a pattern reoccurs with the same orientation and thus scaled by a factor of τ^{12} , *i.e.* ~ 322 . It should be noted that the remaining inequivalent thick rhombs occurring in tilings T_a and T_b do not lead to viable fivefold patterns that can be continued to infinity *via* inflation/deflation.

There is also one infinite twofold tiling associated with each of the tenfold tilings. Although not specifically shown, these tilings are obtained by expanding in the vicinity of the dots in Figs. 6(d)–(f) somewhat below the centers of the fivefold patterns. The respective duals of these patterns are each found to consist of grids based on all three symmetric Fibonacci sequences but in different order. The nuclei of such pentagrids are discernible in the last three pentagrids in Fig. 7.

Discussion

An approach similar to this work, using points of symmetry in a one-dimensional quasiperiodic sequence, would apply to other point symmetries and other dimensions. In particular, there is a straightforward connection with the three-dimensional patterns (Socolar & Steinhardt, 1986) based on the zonohedra that are generated *via* the dual method from hexagrids based on the three Fibonacci sequences along the line t in Fig. 1. Contrary to the present two-dimensional case, each of those sequences leads to singular hexagrids in three dimensions, with the respective dual tilings all belonging to the same local isomorphism class. It is evident that such zonohedral tilings can also be decorated with an Ammann pattern (a hexagrid) which is dual to the tiling itself. They have been called (Socolar & Steinhardt, 1986) the three-dimensional counterparts of the Penrose tilings. Yet they are also perfect three-dimensional analogs of T_c and F_c, F'_c *etc.* Therefore, the formal proofs of the matching rules, inflation/deflation properties *etc.* for the former must hold for the latter by analogy. Moreover, since tilings T_a and T_b *etc.* are decompositions of T_c *etc.* with the same point symmetries, it is not surprising that similar properties also apply to them.

It has been remarked that a singularity in a pentagrid may be removed by slightly shifting its individual Fibonacci grids (de Bruijn, 1981). Such a procedure would certainly decompose a polygon into its constituent rhombs. Yet, clearly, one cannot generate the tilings of the Penrose local isomorphism class in this manner by infinitesimally shifting the grids of the singular pentagrid associated with, for example, tiling T_c . The tilings presented here cannot be considered as decorations of the Penrose tilings.

Some avenues for further study would include the intriguing behavior of a pattern reoccurring after many deflations or inflations, as well as the question of which tiles of the same shape are equivalent. There is also the question of whether these patterns can be obtained *via* projection from some higher-dimensional structure other than hypercubic. In addition, there remains the possible relationship between the tilings described here and the decagonal alloy

phases (Bendersky, 1985) that have been shown to possess tenfold quasiperiodic symmetry in two dimensions, but yet are periodic in the third direction.

APPENDIX

The various Fibonacci pentagrids associated with the tilings discussed earlier are given in Fig. 7. The notation is the same as the corresponding sequences in Fig. 1, where the positive direction is to the right. The pentagrids are formed by orienting grids corresponding to a given sequence along the five principal directions in the plane, of which the first points towards the top of the page. The respective tilings, dual to these pentagrids, are similarly denoted, but capitalized.

Acta Cryst. (1992). **A48**, 541–544

Quantitative Phase Determination from Three-Beam Diffraction with a Corrected Scaling Scheme

BY MAU-TZAI HUANG AND SHIH-LIN CHANG*

Department of Physics, National Tsing Hua University, Hsinchu, Taiwan 30043

(Received 21 October 1991; accepted 28 January 1992)

Dedicated to Professor B. Post on his 80th birthday

Abstract

The scaling scheme in the quantitative phase-determination procedure proposed by Chang & Tang [*Acta Cryst.* (1988), **A44**, 1065–1072] is corrected by taking the average peak intensity of two centrosymmetrically related three-beam diffractions as the maximum kinematical intensity for the reconstruction of the phase-independent intensity profiles. By subtraction of these phase-independent profiles from the measured intensity distributions, more reliable information about phases can be obtained. This procedure is applied to the three-beam diffraction profiles of several organic crystals, reported by Hümmer, Weckert & Bondza [*Acta Cryst.* (1990), **A46**, 393–402], for quantitative phase analysis. The determined phase values are in good agreement with those calculated from the known structures.

1. Introduction

The phase δ of a structure-factor triplet can be determined qualitatively by analyzing the asymmetry of

References

- BENDERSKY, L. (1985). *Phys. Rev. Lett.* **55**, 1461–1463.
 BRUIJN, N. G. DE (1981). *Proc. K. Ned. Akad. Wet. Ser. A*, **84**, 39–52, 53–66.
 CONWAY, J. H. & KNOWLES, K. M. (1986). *J. Phys. A*, **19**, 3645–3653.
 GARDNER, M. (1977). *Sci. Am.* **236**, 110–121.
 GRÜNBAUM, B. & SHEPARD, G. C. (1986). *Tilings and Patterns*. San Francisco: Freeman.
 ISHIHARA, K. N. & YAMAMOTO, A. (1988). *Acta Cryst.* **A44**, 508–516.
 KRAMER, P. & NERI, R. (1984). *Acta Cryst.* **A40**, 580–587.
 LEVINE, D. & STEINHARDT, P. J. (1986). *Phys. Rev. B*, **34**, 596–616, and references therein.
 PENROSE, R. (1974). *Bull. Inst. Math. Appl.* **10**, 266–271.
 SHECHTMAN, D. S., BLECH, I., GRATIAS, D. & CAHN, J. W. (1984). *Phys. Rev. Lett.* **53**, 1951–1953.
 SOCOLAR, J. E. S. (1989). *Phys. Rev. B*, **39**, 10519–10551.
 SOCOLAR, J. E. S. & STEINHARDT, P. J. (1986). *Phys. Rev. B*, **34**, 617–647, and references therein.

the profile tails of the diffracted intensity distribution of a simultaneous three-beam diffraction. That is, $\cos\delta$ can be determined (see, for example, Chang, 1982; Juretschke, 1982; Post, 1983; Gong & Post, 1983; Shen & Colella 1988; and many others). Recently, semiquantitative/quantitative determination of this phase has become feasible (Chang & Tang, 1988; Tang & Chang, 1988; Hümmer, Weckert & Bondza, 1989; Zuo, Spence & Hoier, 1989; Chang, Huang, Tang & Lee, 1989; Weckert & Hümmer, 1990; Hümmer, Weckert & Bondza, 1990) *via* the inspection and analysis of the entire diffraction profiles.

In the phase-determination procedure proposed by Chang & Tang (1988), a three-beam intensity profile is assumed to be composed of a dynamical (phase-dependent) part and a kinematical (phase-independent) part, which are related to the coherent and incoherent contributions, respectively, of this particular diffraction process. To extract phase information from the intensity distribution, the dynamical part ought to be delineated from the measured intensity profile. This can be done by first reconstructing the kinematical part, a Lorentzian, with its width equal to the experimental peak width and its maximum value determined by matching the

* On leave at Corporate Research Science Laboratory, Exxon Research and Engineering, Annandale, New Jersey 08801, USA.